

Large-scale atmospheric circulation changes are associated with the recent loss of Arctic sea ice

By JAMES E. OVERLAND^{1*} and MUYIN WANG², ¹NOAA/Pacific Marine Environmental Laboratory, Seattle, WA 98115, USA; ²JISAO/University of Washington, Seattle, WA 98195, USA

(Manuscript received 14 March 2009; in final form 22 October 2009)

ABSTRACT

Recent loss of summer sea ice in the Arctic is directly connected to shifts in northern wind patterns in the following autumn, which has the potential of altering the heat budget at the cold end of the global heat engine. With continuing loss of summer sea ice to less than 20% of its climatological mean over the next decades, we anticipate increased modification of atmospheric circulation patterns. While a shift to a more meridional atmospheric climate pattern, the Arctic Dipole (AD), over the last decade contributed to recent reductions in summer Arctic sea ice extent, the increase in late summer open water area is, in turn, directly contributing to a modification of large scale atmospheric circulation patterns through the additional heat stored in the Arctic Ocean and released to the atmosphere during the autumn season. Extensive regions in the Arctic during late autumn beginning in 2002 have surface air temperature anomalies of greater than 3 °C and temperature anomalies above 850 hPa of 1 °C. These temperatures contribute to an increase in the 1000–500 hPa thickness field in every recent year with reduced sea ice cover. While gradients in this thickness field can be considered a baroclinic contribution to the flow field from loss of sea ice, atmospheric circulation also has a more variable barotropic contribution. Thus, reduction in sea ice has a direct connection to increased thickness fields in every year, but not necessarily to the sea level pressure (SLP) fields. Compositing wind fields for late autumn 2002–2008 helps to highlight the baroclinic contribution; for the years with diminished sea ice cover there were composite anomalous tropospheric easterly winds of $\sim 1.4 \text{ m s}^{-1}$, relative to climatological easterly winds near the surface and upper tropospheric westerlies of $\sim 3 \text{ m s}^{-1}$. Loss of summer sea ice is supported by decadal shifts in atmospheric climate patterns. A persistent positive Arctic Oscillation pattern in late autumn (OND) during 1988–1994 and in winter (JFM) during 1989–1997 shifted to more interannual variability in the following years. An anomalous meridional wind pattern with high SLP on the North American side of the Arctic—the AD pattern, shifted from primarily small interannual variability to a persistent phase during spring (AMJ) beginning in 1997 (except for 2006) and extending to summer (JAS) beginning in 2005.

1. Introduction

In previous papers we discuss that recent Arctic surface air temperature (SAT), sea level pressure (SLP) and summer sea ice loss often have decidedly different spatial patterns at the beginning of the 21st century compared to most of the 20th century, an Arctic Paradox and suggest calling this recent interval the Arctic Warm period (Overland and Wang, 2005; Overland et al., 2008). In the past we have followed the conceptual model of Quadrelli and Wallace (2004) where, based on Empirical Orthogonal Function (EOF)/Principal Component Analysis of SLP north of 20°N, the main patterns of winter climatic variability are the Arctic Oscillation (AO) and a near approximation to the Pacific North American pattern, labeled PNA*. A recent Arctic

climate pattern is the 3rd EOF mode of SLP north of 20°N, and has been referred to as the third Arctic pattern, a Dipole pattern, the Arctic Warm pattern, the Barents Oscillation or the meridional pattern, as it contrasts to the more zonal pattern of the AO (Skeie, 2000; Overland and Wang, 2005; Zhang et al., 2008). Several authors relate the recent major reduction in summer Arctic sea ice extent in part to the presence and phasing of this meridional atmospheric climate pattern, which resulted in a much faster than the expected loss of sea ice in the real world compared to the timing of ensemble mean projections found in climate models based on anthropogenic forcing alone (e.g. Wu et al., 2006; Maslanik et al., 2007; Stroeve et al., 2007; Holland et al., 2008; L'Heureux et al., 2008; Wang et al., 2009). Current usage supports calling this pattern the Arctic Dipole (AD).

Most authors including the present ones considered that the persistent AO and AD patterns were mainly representative of natural variability of the chaotic climate system in the northern latitudes. However, due to recent sea ice loss at the end

*Corresponding author.

e-mail: james.e.overland@noaa.gov

DOI: 10.1111/j.1600-0870.2009.00421.x

of summer there is a direct feedback to shifts in the broader atmospheric circulation in late autumn and winter. Heat being stored in the upper Arctic Ocean due to reduction in the area of Arctic summer sea ice is given back to the atmosphere in the following autumn, which has a direct impact on the temperature of the troposphere (Schweiger et al., 2008; Serreze et al., 2009) and thus on geopotential height and thickness fields. Chapman and Walsh (2007) based on Intergovernmental Panel on Climate Change (IPCC) models, Singarayer et al. (2006) based on the Hadley Center climate model, and Francis et al. (2009) based on the NCEP/NCAR Reanalysis (NNR) suggest that regional loss of sea ice can have hemispheric consequences in atmospheric circulation. Sokolova et al. (2007), Seierstad and Bader (2008) and Honda et al. (2009) show a relation in models between years with minimum sea ice cover and the negative phase of the AO (weaker zonal wind), although regional details are complicated by storm track and atmospheric long-wave/low-frequency dynamic processes. Thus model results and recent atmospheric conditions suggest that the continued reduction of sea ice in summer and other Arctic climate changes are not simply be due to natural chaotic and anthropogenic processes alone, but include an important feedback component to the atmospheric circulation mediated by sea ice loss and forcing from the surface.

We investigate recent observations for evidence of variations in the frequency of climate patterns in the Arctic and for potential atmospheric impacts from reductions in summer Arctic sea ice cover. In the next section we evaluate the persistence and seasonality of the AO and AD patterns more completely than has been done previously. In Section 3, the main part of the paper, we document the late autumn (OND) tropospheric temperature and dynamic impact through the geopotential height and 500–1000 hPa thickness fields associated with reduced summer sea ice cover during recent years in the western (Pacific side) Arctic.

2. AO and AD climatology

We make use of a limited area EOF analysis to compare seasonal time series of the more zonal AO pattern with the more meridional AD pattern. To put this regional analysis into physical context, we begin by showing the standard first three EOF patterns of individual months from the extended winter season (NDJFM) for SLP anomaly fields over nearly the entire northern hemisphere (north of 20°N) from 1959 to 1998, based on the NNR (Fig. 1 left-hand panel). The first three patterns are the AO and the PNA* as discussed by Quadrelli and Wallace (2004) and the more meridional ‘third’ pattern across the central Arctic discussed by Overland and Wang (2005). Sign conventions are arbitrary, but the positive phase of the AO is considered to be associated with a negative SLP anomaly over the central Arctic and the third or AD pattern has a dipole field with the positive phase associated with a negative SLP anomaly on the North American side of the Arctic.

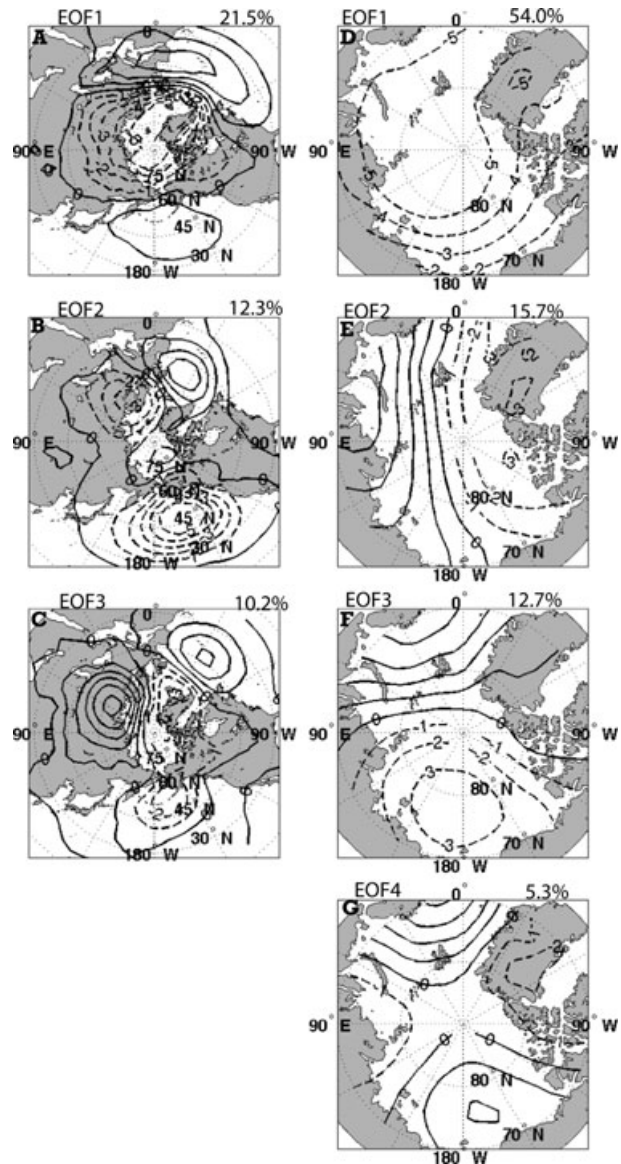


Fig. 1. Extended winter (NDJFM) EOF patterns of sea level pressure (SLP) for the 1959–1998 period based on NCEP/NCAR reanalysis fields over 20–90°N (left-hand panels) and 70–90°N (right-hand panels). Fields have been converted to SLP units with contour intervals of 1 hPa. Note the similarities between EOF3 of 20–90°N (c), and the EOF2 of 70–90°N (e).

EOFs are designed to capture the most variance in a times series of spatial fields subject to the mathematical constraint that the EOFs are mathematically orthogonal. An added concern is that as the spatial correlation length of the physical field approaches the size of the spatial domain, the boundaries also impose pattern preferences on the EOF patterns. If the region is too small, the first four EOFs show a drumhead, two orthogonal dipole patterns and a saddle pattern, the so called Buell patterns (Legates, 1993), in addition to any physical content. Based on an

EOF application for SLP by Kutzbach (1970) and others, it was realized that boundary influences in hemispheric SLP or 500 hPa geopotential height EOF analyses would not be an issue as the correlation length of the geostrophic wind is reduced approaching the Equator. Thus the first two patterns in Fig. 1 left-hand panel are rather robust as ‘climate’ patterns and are also seen in other types of analyses such as single point correlations and regional indices (Quadrelli and Wallace, 2004). The third pattern shows some sensitivity in its spatial detail for analyses based on data from the first versus the second half of the 20th century (Overland and Wang, 2005).

In the current paper we focus on the Arctic. The right-hand panels of Fig. 1 show a limited region EOF analysis of individual months for extended winter (NDJFM) SLP anomalies north of 70°N. As expected, because the SLP correlation length is comparable to the size of the Arctic basin, the limited area EOF patterns show boundary influences with the characteristic Buell patterns. Even though the EOFs in Fig. 1 right-hand panel cannot be considered independent climate patterns compared to those in Fig. 1 Left-hand panel, we can make use of the principal components (PCs) of these regional Arctic EOFs, because the first regional EOF (EOF1) has a local resemblance to the hemispheric AO (PC correlation of 0.96) and regional EOF2 has a resemblance to the third EOF-AD pattern (PC correlation of 0.77) of

the hemispheric analysis. Thus the physical justification for the use of the limited area patterns and PCs comes from the comparison to the hemispheric analysis. However, we expect a better set of basis functions from the reduced area patterns for projecting seasonal data, as these patterns are based on the limited region. This physical justification also applies the limited area analysis of Wang et al. (2009). Our EOF3 has a resemblance to the second EOF/dipole pattern of Wu et al. (2006) and Wang et al. (2009) where the geostrophic winds are oriented on an Alaskan/Kara Sea axis. Our EOF2 and the Wang et al. (2009) summer dipole pattern are oriented more with Fram Strait. Because of the Buell pattern relationships, a linear combination of the regional EOF2 and EOF3 can represent the dipole /meridional pattern with all possible orientations.

Figure 2 shows the regression coefficients of the SLP anomaly fields projected onto the first two limited area EOFs for the four seasons (OND, JFM, AMJ and JAS); we use these seasonal divisions to be consistent with our analyses in the next section. Bars show the values of PC1 and the continuous line are the magnitudes of PC2; both time series are normalized by their seasonal standard deviation for 1948–2008. PC1 shows the well-known positive values of the AO in winter from 1989 to 1997 and variable values after that. There are also positive values for the AO in late autumn for 1988–1994. PC2, the meridional AD pattern,

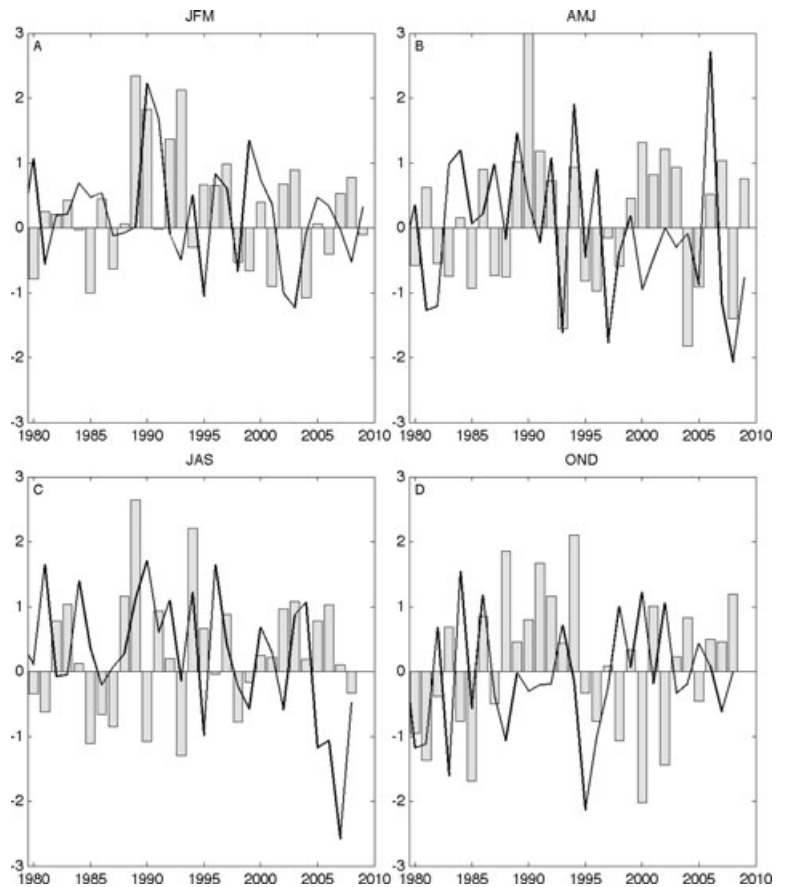


Fig. 2. Seasonal mean Principal Components (PC) of corresponding first two EOFs for 70–90°N. The PC1 (AO) is shown by vertical bars, and PC2 (AD) is shown by solid lines for 1980–2008. The PCs are the monthly SLP anomalies regressed to EOF spatial patterns shown in the right-hand panels of Fig. 1, and then averaged for each season. Both time-series are normalized by their standard deviation for 1948–2008.

has a run of negative values during spring beginning in 1997 to the present with the exception of 2006. Negative PC2 has a positive SLP anomaly in the Beaufort Sea region and negative SLP anomalies on the Siberian side of the Arctic Basin; this provides anomalous geostrophic winds flowing from the Bering Strait region toward the North Pole as in summer 2007. The extreme negative value of PC2 (AD) in summer 2007 is clearly seen with a standard deviation of 2.5 (Fig. 2c), which directly contributed to the major reduction in September sea ice extent in that year. The same negative phase, but with smaller magnitude, was also present in 2005 and 2006. Our results show decadal shifts in principal Arctic climate patterns similar to Wang et al. (2009), although we place more emphasis on the AD shifts during recent springs.

3. Tropospheric temperature and wind impact from loss of September sea ice

We now shift to the potential impacts of reduction of summer sea ice extent on late autumn atmospheric conditions and begin by examining the late autumn (OND) air temperature fields in recent years with reduced September sea ice cover. Extensive open water areas are seen during September in the Chukchi Sea in 1999 and again beginning in 2002–2008 relative to earlier years (NSIDC website http://nsidc.org/data/seaiice_index/). An extensive area of open water was seen in the East Siberian Sea in 2005 and 2006. Air temperature anomalies at 1000 hPa over the central and Pacific Arctic show extensive late autumn anomalies of +2 °C beginning in 1995, +4 °C beginning in 2002 and +6 °C for 2007 and 2008, relative to a base period of 1968–1996 as obtained from the NNR (<http://www.cdc.noaa.gov/>). These temperature anomaly fields for 2002–2005 and 2007–2008 are shown in Fig. 3. The base period used by CDC is different from our normal period used in our previous section, which is unfortunate. However, since this CDC analysis tool is widely used by the community, we feel that is better to be consistent with the CDC normal period instead of recalculating the anomalies relative to a 1959–1998 period mean; the differences between the two anomaly patterns based on the different normal periods are small (figures not shown). The late autumn air temperature cross-section from 60°N to 90°N over the western Arctic (from 135°E to 225°E longitude) averaged over 2002–2008 is shown in Fig. 4. In this composite, the large near SAT anomalies are present and 1 °C anomalies occur above the 850 hPa level. The temperature anomaly cross-section fields for all years in this composite are qualitatively the same, but in the years 2003, 2004 and 2008, the level of the 1 °C contour is restricted to below 800 hPa.

One may have some concern about the reliability of the NNR and other Reanalysis fields over the central Arctic as there are no direct rawinsonde vertical temperature profiles over the Arctic Ocean. This is also an issue for the recent Schweiger et al. (2008), Serreze et al. (2009), and Francis et al. (2009) papers. First, sev-

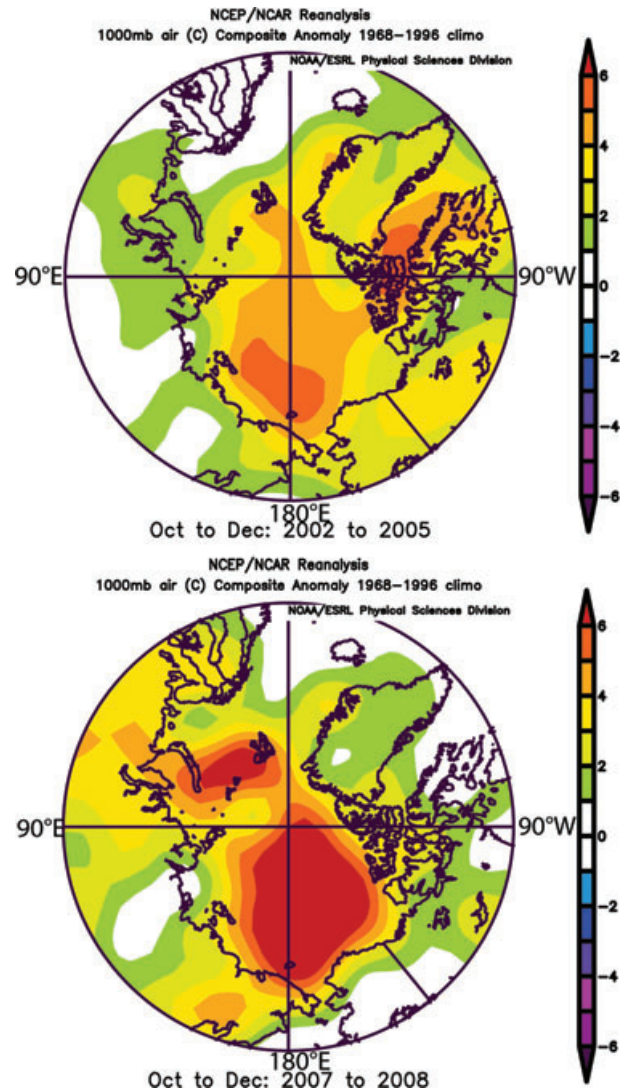
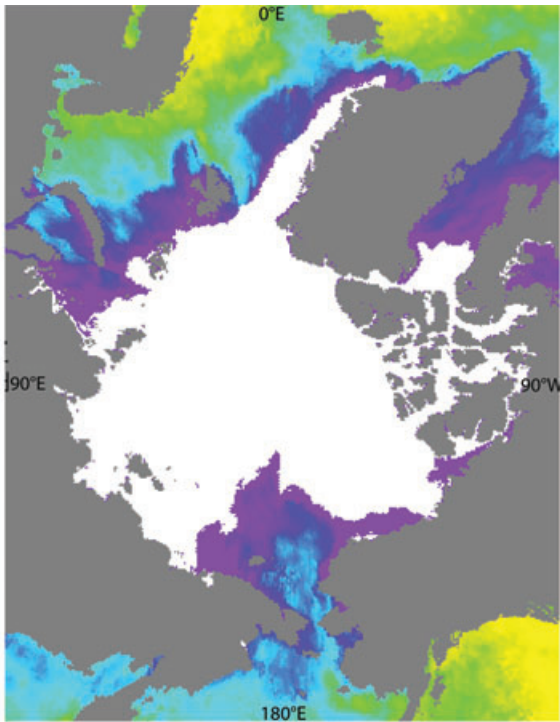
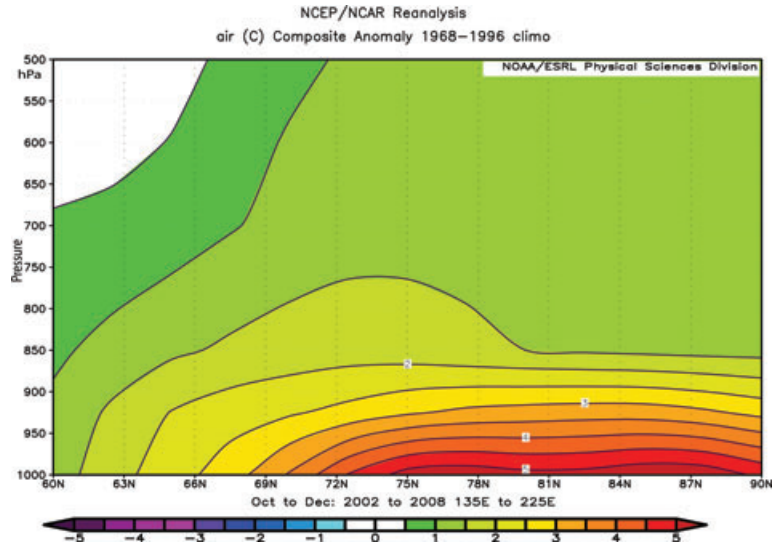


Fig. 3. Near surface air temperature anomaly multiyear composites (°C) for (top panel) October–December 2002–2005 and (bottom panel) October–December 2007–2008, the 2 yr with extreme minimum September sea ice extents. Anomalies are relative to 1968–1996 mean. Data are from the NCEP–NCAR Reanalysis through the NOAA/Earth Systems Research Laboratory, generated online at www.cdc.noaa.gov.

eral coastal stations such as Barrow AK, show such temperature anomalies. Second, the values of 2007–2008 late autumn near surface temperatures in the northern Beaufort Sea in the NNR are approximately -15°C compared to the long-term mean values of approximately -20°C , providing anomalies of approximately $+5^{\circ}\text{C}$. Such a relative shift in the NNR temperatures is plausible given the recent summer and autumn sea ice conditions. Figure 5 for example, is the sea surface temperature analysis for 31 October 2007, based on a blend of MODIS and AMSER-E satellite data, which shows above freezing temperatures for much of the Chukchi Sea well into autumn. Further based on

Fig. 4. The vertical cross-section composite plot of air temperature anomalies ($^{\circ}\text{C}$) for the section covering East Siberia Sea, Chukchi Sea and Beaufort Sea ($135\text{--}225^{\circ}\text{E}$) from Bering Strait ($\sim 60^{\circ}\text{N}$) to the North Pole (90°N) for October–December 2002–2008.



SST:
 -1 4 9 14 19 24 29
 (degrees Celsius)

Fig. 5. Sea surface temperature field for 31 October 2007 from MODIS and AMSER-E-satellite data (http://www.remss.com/sst/sst_data_daily.html?sat = mw_ir).

satellite data, Giles et al. (2008) and Kwok et al. (2009) show a removal or thinning of multiyear sea ice in recent years for most of the Arctic away from Greenland/Canadian North. Perovich et al. (2008) shows thin ice in the northern Beaufort Sea for sea

ice that did not completely melt out based on in situ sea ice mass balance buoys. These results contrast with historical observations that sea ice in the central Beaufort Sea begins freeze up during September. With regard to temperature increases above the surface Schweiger et al. (2008) make a case that the normal stable stratification of the Arctic radiatively maintained boundary layer (Overland and Guest, 1991) is eroded by warm temperatures from the surface. Further we do not see strong temperature advection over the Pacific Arctic in autumn 2007 or 2008 relative to surface contributions (analysis not shown). Yearly temperature shifts in the NNR also qualitatively hold for the JRA-25 Reanalysis. Surface temperatures are $\sim 2^{\circ}\text{C}$ warmer in the NNR relative to the JRA-25, but above this level the magnitudes and patterns are similar with the NNR being about $\sim 0.3^{\circ}\text{C}$ warmer throughout the troposphere relative to the JRA-25. Our results are in agreement with a similar analysis carried out by Serreze et al. (2009). Thus our only concern is that the NNR autumn surface temperatures, while having qualitatively consistent warm anomalies, could have too great a magnitude. The reanalysis comparison is carried out for the temperature fields as all other dynamic fields, for example, thermal wind, are based primarily on temperature. Based on the preceding antidotal information, it is not unreasonable to expect on physical grounds a qualitative relative increase in Arctic tropospheric temperatures and impacts on further derived dynamic fields for recent years as shown in the NNR compared to the NNR climatology.

The corresponding 1000–500 hPa anomalous thickness field for late autumn 2002–2008 is shown in Fig. 6. All years contribute to the composite values in the Pacific Arctic, while the thickness anomaly maximum over Spitzbergen is primarily a feature of 2005 and 2006. Given the persistent magnitudes and location of the late autumn thickness anomalies and their gradients over the Pacific Arctic in years of minimum sea ice cover, and the connection through heat storage in the ocean and erosion of the atmospheric boundary layer stratification (Schweiger

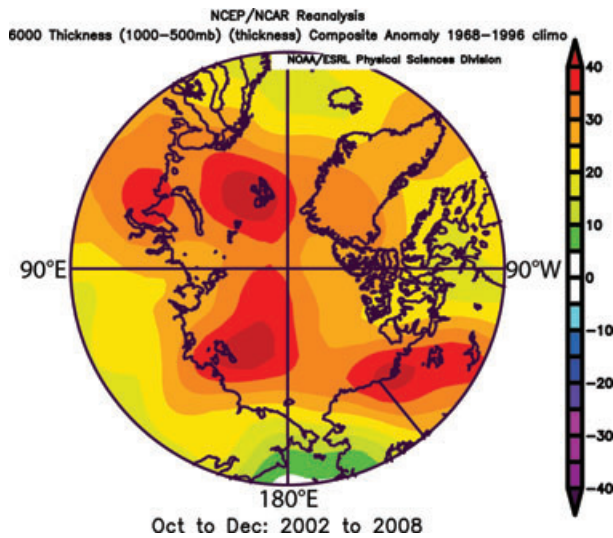


Fig. 6. The 1000–500 hPa thickness field anomaly composite for October–December 2002–2008. Note the band of greater thickness from the East Siberian Sea to northern Alaska, the region of diminished September sea ice cover that has a contribution from every year. The local maximum over Spitzbergen is a feature for 2005 and 2006.

et al., 2008), one can infer an impact on the atmospheric circulation directly related to late autumn surface temperature anomalies and earlier sea ice loss.

Dynamical quantities such SLP, geopotential heights and zonal and meridional wind fields show much more year to year variability for late autumns (OND) of 2002–2008 than the air temperature and thickness fields. They not only contain the influence of the baroclinic contribution from gradients in the 1000–500 hPa thickness fields but also a barotropic contribution that reflects the interannual variability of the atmospheric upper level polar vortex (Thompson et al., 2000; Angell, 2006) and other contributions. Thus the late autumn SLP fields (not shown) resemble an AD pattern in 2002, 2003, 2005 and 2006,

a weak AO pattern in 2004 and 2007, and a positive AO pattern in 2008. The mutual contributions from the baroclinic and barotropic components to the atmospheric circulation field make it difficult to assign a clear contribution to the total wind field anomalies from summer loss of sea ice in any one yr.

Because we expect a contribution from a positive poleward gradient in thickness from the loss of September sea ice in every year from 2002 to 2008, compositing dynamic quantities over these years should expose a persistent wind field impact primarily due to a reduction in sea ice extent. Figure 7 is the cross-section plot of geopotential height anomalies corresponding to the air temperature anomaly cross-section in Fig. 4. There is clearly a south–north gradient in geopotential heights anomaly at all levels in the lower troposphere over the Pacific Arctic in late autumn. This gradient opposes the climatological geopotential height gradient which favors westerly zonal wind flow associated with the polar vortex. Figure 8 is the corresponding October–December 2002–2008 geopotential height anomaly field at 850 hPa showing the positive anomaly over the Pacific Arctic. The spatial pattern of the anomaly field is similar to the composite 850 hPa height field for 2002–2008, with a strengthening of the Beaufort High at 850 hPa and polar easterlies near the Alaskan coast relative to the CDC/NNR climatology. In the composite we see no strong indication of a major contribution from horizontal advection to the central Beaufort tropospheric temperature anomalies in these composite 850 height fields relative to a local surface heat source. Serreze et al. (2009) does suggest a role for advection in recent years; they include September in their composite, while we include December, a time when the late autumn Beaufort High pattern is more established. There also is year-to-year and monthly variability in the advection fields that is suppressed in the compositing.

The corresponding zonal wind field anomaly cross-section for October–December 2002–2008 (Fig. 9) is shown in solid (positive) and dashed (negative) contours, relative to the CDC/NNR climatological zonal wind (colour shading). The anomaly is

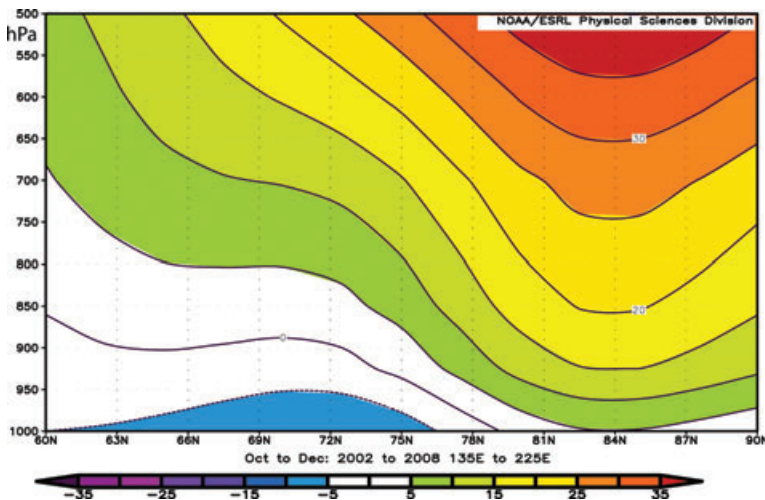


Fig. 7. The vertical cross-section composite plot of geopotential height anomalies (dynamic meters) for the section from Bering Strait (60°N) to the North Pole (90°N) for October–December 2002–2008 over the area from Siberia Sea to Beaufort Sea (135–225°E).

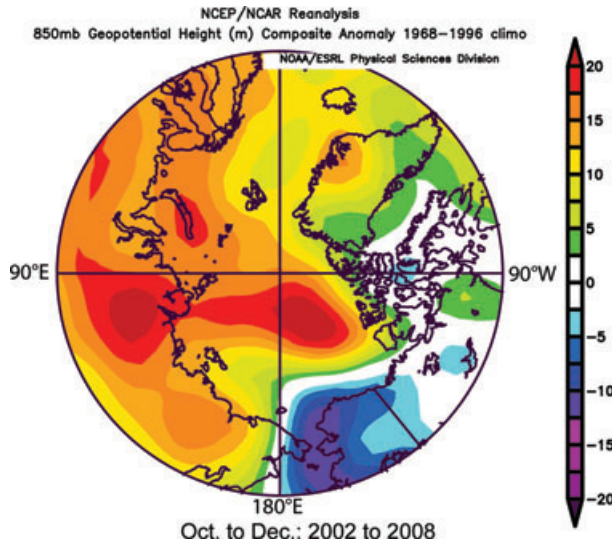


Fig. 8. The 850 hPa geopotential height anomaly composite for October–December 2002–2008. Note the relative high over the northern Beaufort Sea.

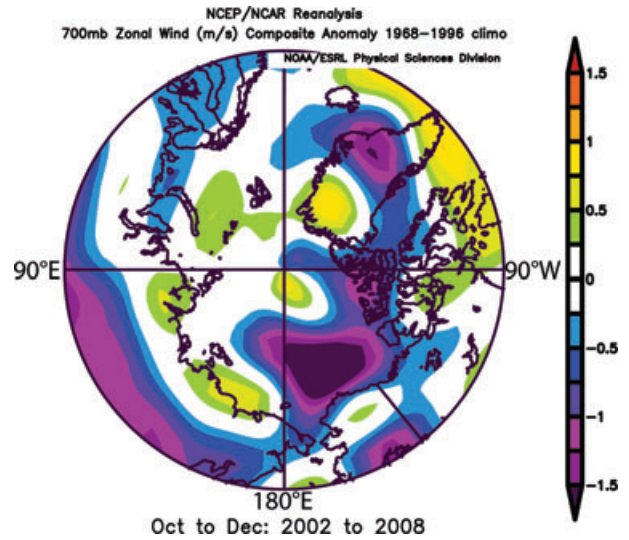


Fig. 10. Zonal wind anomaly composite (m s^{-1}) at 700 hPa for October–December 2002–2008. Note the reduction in the zonal wind component north of Alaska and western Canada.

negative with a magnitude of $\sim 1.2 \text{ m/s}$ starting above the surface and extending throughout the troposphere. Figures 7–9 show that the major baroclinicity was in the lower troposphere. The magnitude of the zonal wind anomaly compares to a climatological $\sim 3 \text{ m s}^{-1}$ magnitude of the near surface polar easterly to the south and the upper tropospheric westerly to the north. The effect of the anomaly is to increase the magnitude of the polar easterly and shift it to the north, while reducing the upper level westerly. Figure 10 shows a negative value for the composite anomalous zonal wind component on the 700 hPa surface for late autumn 2002–2008 extending from Bering Strait eastward north of Alaska and the Canadian Archipelago. The anomalous

zonal wind component during autumn for the recent sea ice free years represents 40% of the magnitude of the maximum climatological wind speeds.

4. Discussion and conclusions

The AD climate pattern, which has a more meridional anomalous wind pattern compared to the more zonal wind pattern of the AO, occurs more frequently in its negative phase in the 21st century compared to the late 20th century. Increased persistence is clear in spring and more recently in summer. These recent years are associated with a reduction in the extent of September sea ice

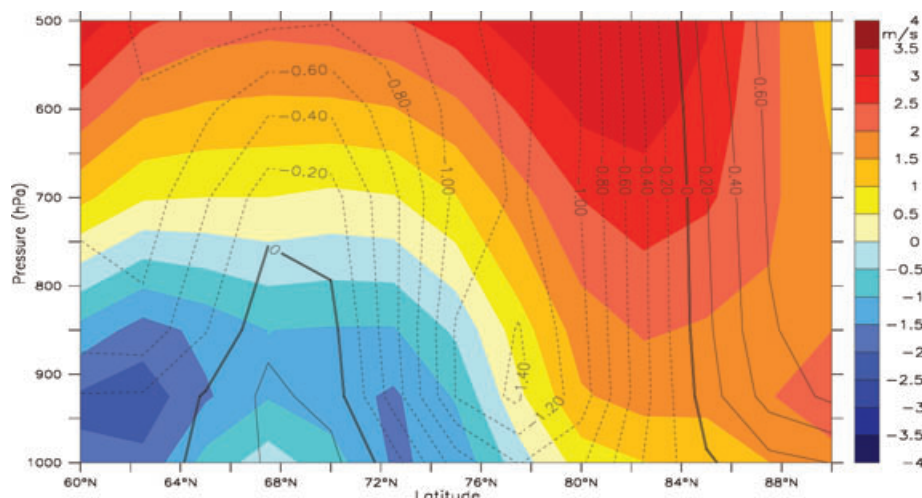


Fig. 9. The vertical cross-section composite plot of the zonal wind anomalies (dashed and solid contours in m s^{-1}) for the section from Bering Strait ($\sim 60^\circ\text{N}$) to the North Pole (90°N) for October–December 2002–2008 over the area from Siberia sea to Beaufort Sea ($135\text{--}225^\circ\text{E}$). The corresponding climatological zonal wind field is shown in colour shading; the climatological period is 1968–1996, the period used by CDC.

cover in the Arctic and further support the claim of Wang et al. (2009) that the shift toward more of meridional/AD pattern in the Arctic was not only important in the summer of 2007 (L'Heureux et al., 2008), but also had a role in the preconditioning of the sea ice loss over the previous decade (Fig. 2b). Thus, sea ice advection in the early 1990s with the positive AO was not the only factor in the preconditioning of the 2007 minimum summer sea ice extent (Rigor and Wallace, 2004).

The most important conclusion of this and several recent papers is that the loss of summer Arctic sea ice can have an impact on the larger Northern Hemisphere atmospheric circulation. We show increased air temperatures in the lower troposphere over the Arctic in late autumn (OND), similar to the analysis of Serreze et al. (2009) for (SON), and thus a delayed north–south gradient in the 1000–500 hPa thickness field associated with a reduction in September sea ice cover. This connection is mediated by heat storage in the ocean (Fig. 5) and an erosion of the stable Arctic boundary layer from the surface (Schweiger et al., 2008). While we saw a positive anomaly in the thickness field in every year with extensive September open water, there is considerable year-to-year variability in pressure fields. The fields of SLP are more complicated as they are also impacted by a barotropic contribution from the polar vortex and by mid-latitude influences (Francis et al., 2009). Unlike the thickness fields, one should not expect a direct correspondence between loss of sea ice and the SLP field in every year.

The consequences of increased September open water in the western Arctic and increased 1000–500 hPa thickness is an anomalous late autumn easterly zonal wind component, especially north of Alaska and Canada on the order of 40%. This could be interpreted as a diminished contribution to the large scale wind pattern from the positive AO, and support for the AD and more regional variability. Consequences for mid-latitude weather from a more meridional flow pattern associated with sea ice reduction can be complex involving storm track/long-wave interactions (Singarayer et al., 2006, Sokolova et al., 2007; Seierstad and Bader 2008). Cold air can move south as in the Eurasian teleconnection example of Honda et al. (2009). Such northern mid-latitude impacts will increase as the current sea ice reduction of 38% compared to climatology increases to 80% over the next decades (Wang and Overland, 2009).

A combination of modest anthropogenic forcing and the recent presence of the positive AO and negative AD, acting through the loss of summer sea ice and increased autumn temperatures, have induced further changes in the atmospheric circulation at an earlier date than anticipated from anthropogenic contributions alone. Whether the reduction in Arctic sea ice may have increased the frequency of the AD due to positive feedbacks in the sea ice/ocean/atmospheric climate system is difficult to determine authoritatively from data, given confounding contributions of the barotropic and baroclinic contributions to the flow field in the last decade. However, as summer Arctic open water area increases over the next decades, we anticipate an increasing

influence of loss of summer sea ice on the atmospheric northern hemisphere general circulation in following seasons. Thus, while the magnitude of the direct effect of anthropogenic forcing to climate change is still emerging, it may already have shifted the normal chaotic patterns of natural climate variability in the sub-Arctic through sea ice/ocean feedbacks and contributed to an accelerated arctic amplification of temperature.

5. Acknowledgments

We appreciate the support of NOAA Arctic Research of the Climate Program Office. We have enjoyed discussions of this topic with many colleagues over the last 2 yr, and thank James Maslanik for discussion of available SST fields for the Arctic and Donald Perovich for discussion of the ice mass buoy data. This publication is partially funded by the Joint Institute for the Study of the Atmosphere and Ocean (JISAO) under NOAA Cooperative Agreement No. NA17RJ1232, Contribution #1758. PMEL Contribution #3202.

References

- Angell, J. K. 2006. Changes in the 300-mb North Circumpolar Vortex, 1963–2001. *J. Climate* **19**, 2984–2994.
- Chapman, W. L. and Walsh, J. E. 2007. Simulations of Arctic temperature and pressure by global coupled models. *J. Climate* **20**, 609–632.
- Francis, J. A., Chan, W., Leathers, D. J., Miller, J. R. and Veron, D. E. 2009. Winter Northern Hemisphere weather patterns remember summer Arctic sea ice extent. *Geophys. Res. Lett.* **36**, L07503, doi:10.1029/2009GL037274.
- Giles, K. A., Laxon, S. W. and Ridout, A. L. 2008. Circumpolar thinning of Arctic sea ice following the 2007 record ice extent minimum. *Geophys. Res. Lett.* **35**, L22502, doi:10.1029/2008GL035710.
- Holland, M. M., Bitz, C. M., Tremblay, B. and Bailey, D. A. 2008. The role of natural versus forced change in future rapid summer Arctic ice loss. In: *Arctic Sea Ice Decline: Observations, Projections, Mechanisms, and Implications Geophys. Monogr. Ser. 180* (eds E. T. DeWeaver, C. M. Bitz and L. B. Tremblay). AGU, Washington, DC, 133–150.
- Honda, M., Inoue, J. and Yamane, S. 2009. Influence of low Arctic sea ice minima on anomalously cold Eurasian winters. *Geophys. Res. Lett.* **36**, L08707, doi:10.1029/2008GL037079.
- Kutzbach, J. 1970. Large-scale features of monthly mean Northern Hemisphere anomaly maps of sea-level pressure. *Mon. Wea. Rev.* **98**, 708–716.
- Kwok, R., Cunningham, G. F., Wensnahan, M., Rigor, I., Zwally, H. J. and co-authors. 2009. Thinning and volume loss of the Arctic Ocean sea ice cover: 2003–2008. *J. Geophys. Res.* **114**, C07005, doi:10.1029/2009JC005312.
- Legates, D. R. 1993. The effect of domain shapes on principal components analysis: a reply. *Int. J. Climatol.* **13**, 219–228.
- L'Heureux, M. L., Kumar, A., Bell, G. D., Halpert, M. S. and Higgins, R. W. 2008. Role of the Pacific–North American (PNA) pattern in the 2007 Arctic sea ice decline. *Geophys. Res. Lett.* **35**, L20701, doi:10.1029/2008GL035205.
- Maslanik, J., Drobot, S., Fowler, C., Emery, W. and Barry, R. 2007. On the Arctic climate paradox and the continuing role of atmospheric

- circulation in affecting sea ice conditions. *Geophys. Res. Lett.* **34**, L03711, doi:10.1029/2006GL028269.
- Overland, J. E. and Guest, P. S. 1991. The Arctic snow and air temperature budget over sea ice during winter. *J. Geophys. Res.* **96**, 4651–4662.
- Overland, J. E. and Wang, M. 2005. The third Arctic climate pattern: 1930s and early 2000s. *Geophys. Res. Lett.* **32**, L23808, doi:10.1029/2005GL024254.
- Overland, J. E., Wang, M. and Salo, S. 2008. The recent Arctic warm period. *Tellus* **60A**, 589–597.
- Perovich, D. K., Richter-Menge, J. A., Jones, K. F. and Light, B. 2008. Sunlight, water, and ice: extreme Arctic sea ice melt during the summer of 2007. *Geophys. Res. Lett.* **35**, L11501, doi:10.1029/2008GL034007.
- Quadrelli, R. and Wallace, J. M. 2004. A simplified linear framework for interpreting patterns of Northern Hemisphere wintertime climate variability. *J. Climate* **17**, 3728–3744.
- Rigor, I. G. and Wallace, J. M. 2004. Variations in the age of Arctic sea-ice and summer sea-ice extent. *Geophys. Res. Lett.* **31**, L09401, doi:10.1029/2004GL019492.
- Schweiger, A. J., Lindsay, R. W., Vavrus, S. and Francis, J. A. 2008. Relationships between Arctic sea ice and clouds during autumn. *J. Climate* **21**, 4799–4810.
- Seierstad, I. A. and Bader, J. 2008. Impact of a projected future Arctic Sea Ice reduction on extratropical storminess and the NAO. *Clim. Dyn.* **33**, 937–943.
- Serreze, M. C., Barrett, A. P., Stroeve, J. C., Kindig, D. N. and Holland, M. M. 2009. The emergence of surface-based Arctic amplification. *The Cryosphere* **3**, 11–19.
- Singarayer, J. S., Bamber, J. L. and Valdes, P. J. 2006. Twenty-first-century climate impacts from a declining Arctic sea ice cover. *J. Climate* **19**, 1109–1125.
- Skeie, P. 2000. Meridional flow variability over the Nordic Seas in the Arctic Oscillation framework. *Geophys. Res. Lett.* **27**, 2569–2572.
- Sokolova, E., Dethloff, K., Rinke, A. and Benkel, A. 2007. Planetary and synoptic scale adjustment of the Arctic atmosphere to sea ice cover changes. *Geophys. Res. Lett.* **34**, L17816, doi:10.1029/2007GL030218.
- Stroeve, J., Holland, M. M., Meier, W., Scambos, T. and Serreze, M. 2007. Arctic sea ice decline: faster than forecast. *Geophys. Res. Lett.* **24**, L09501, doi:10.1029/2007GL029703.
- Thompson, D. W. J., Wallace, J. M. and Hegerl, G. C. 2000. Annular modes in the extratropical circulation. Part II: trends. *J. Climate* **13**, 1018–1036.
- Wang, J., Zhang, J., Watanabe, E., Ikeda, M., Mizobata, K. and co-authors. 2009. Is the Dipole Anomaly a major driver to record lows in Arctic summer sea ice extent? *Geophys. Res. Lett.* **36**, L05706, doi:10.1029/2008GL036706.
- Wang, M. and Overland, J. E. 2009. A sea ice free summer Arctic within 30 years? *Geophys. Res. Lett.* **36**, L07502, doi:10.1029/2009GL037820.
- Wu, B., Wang, J. and Walsh, J. E. 2006. Dipole Anomaly in the winter Arctic atmosphere and its association with sea ice motion. *J. Climate* **19**, 210–225.
- Zhang, X., Sorteberg, A., Zhang, J., Gerdes, R. and Comiso, J. C. 2008. Recent radical shifts of atmospheric circulations and rapid changes in Arctic climate system. *Geophys. Res. Lett.* **35**, L22701, doi:10.1029/2008GL035607.